

## Comparison of Al<sub>2</sub>O<sub>3</sub>- and AlPO<sub>4</sub>-coated LiCoO<sub>2</sub> cathode materials for a Li-ion cell

Jaephil Cho<sup>a</sup>, Tae-Gon Kim<sup>b</sup>, Chunjoong Kim<sup>b</sup>, Joon-Gon Lee<sup>b</sup>,  
Young-Woon Kim<sup>b</sup>, Byungwoo Park<sup>b,\*</sup>

<sup>a</sup> Department of Applied Chemistry, Kumoh National Institute of Technology, Gumi, Republic of Korea

<sup>b</sup> School of Materials Science and Engineering, and Research Center for Energy Conversion and Storage, Seoul National University, Seoul, Republic of Korea

Available online 26 April 2005

### Abstract

The electrochemical and thermal properties of AlPO<sub>4</sub>-coated LiCoO<sub>2</sub> were compared with those of the Al<sub>2</sub>O<sub>3</sub>-coated cathode. Even though cycling stability of the Al<sub>2</sub>O<sub>3</sub>-coated cathode was apparently similar to that of the AlPO<sub>4</sub>-coated sample at 4.6 V cycling, increasing the charge-cutoff voltage to 4.8 V led to the rapid capacity decay, exhibiting ~20% larger capacity-fading than the AlPO<sub>4</sub>-coated cathode. The irreversible capacity of the Al<sub>2</sub>O<sub>3</sub>-coated cathode (~34 mAh g<sup>-1</sup>) was also larger than that of AlPO<sub>4</sub>-coated cathode (~24 mAh g<sup>-1</sup>) at a charge-cutoff voltage of 4.8 V. This was attributed to the increase in the amount of Co dissolution into the electrolyte at higher voltage. Differential scanning calorimetry results showed that the overall exothermic-heat release of the Al<sub>2</sub>O<sub>3</sub>-coated cathode was similar to that of the bare cell, but the onset temperature of oxygen evolution from the cathode was increased to ~190 °C (up from ~170 °C in the bare cell). On the other hand, AlPO<sub>4</sub>-coated LiCoO<sub>2</sub> showed a much improved onset temperature of the oxygen evolution at ~230 °C, and a much lower amount of exothermic-heat release, compared to the Al<sub>2</sub>O<sub>3</sub>-coated sample. These results were correlated with the 12 V overcharge experiments: the Li-ion cell containing AlPO<sub>4</sub>-coated LiCoO<sub>2</sub> did not show a thermal runaway behavior in contrast to that containing bare, or Al<sub>2</sub>O<sub>3</sub>-coated cathode.

© 2005 Elsevier B.V. All rights reserved.

**Keywords:** AlPO<sub>4</sub> coating; Al<sub>2</sub>O<sub>3</sub> coating; LiCoO<sub>2</sub>; Cycling stability; Co dissolution; Overcharge

### 1. Introduction

The most critical factors for evaluating the performance of Li-ion cells are the rate capability, the cycle life, and the thermal stability, which are mostly affected by the cathode materials. Among them, the thermal stability of the cell becomes more important factor as the cell capacity increases. The cells without protective devices shows the thermal runaway inducing the over-current, over-charge, and abrupt temperature increase during the 12 V overcharging test recommended by the safety guidelines [1,2]. Many safety accidents of Li-ion cells due to the malfunction of the devices in mobile electronics have been reported [3]. The increase in the weight

portion of the cathode accelerated the heat-accumulation rate, and an internal short circuit resulted in a cell explosion with the external temperature exceeding ~500 °C [4].

The most detrimental factor causing such problems is the violent exothermic reaction of the delithiated cathode materials with the flammable electrolytes at elevated temperatures. Its effect has been widely evaluated using differential scanning calorimetry (DSC) and accelerating rate calorimetry as a function of temperature [5–9]. Several authors have reported that additives in the electrolytes can prevent thermal runaway [10–14]. However, they reported that the additives, such as phosphorus compounds or aromatic compounds with two methyl groups, could reduce the flammable nature of the electrolytes.  $\gamma$ -Butyrolactone was used to reduce the direct reaction of the cathode with the electrolyte at the charged state, and this solvent has been reported to decompose into the organic products, which encapsulate the cathode and block any

\* Corresponding author. Tel.: +82 2 880 8319; fax: +82 2 883 8197.

E-mail addresses: [jpcho@kumoh.ac.kr](mailto:jpcho@kumoh.ac.kr) (J. Cho),  
[byungwoo@snu.ac.kr](mailto:byungwoo@snu.ac.kr) (B. Park).

direct reaction with the electrolytes [10]. As a consequence, Li-ion cells containing this solvent did not explode during a nail penetration test at 4.35 V. However, these additives damaged the electrochemical properties of the cathode and anode materials.

Recently, Cho et al. used a fundamental approach to minimize the thermal instability of the cathode materials by an  $\text{AlPO}_4$  nanoparticle coating [5]. Li-ion cells containing the coated cathodes showed no thermal runaway with a maximum cell external temperature of  $\sim 60^\circ\text{C}$  up to 12 V charging in contrast to that containing the bare cathode showing the external temperature of over  $\sim 500^\circ\text{C}$ . This study further reported that the thermal runaway occurred immediately after the internal short at 12 V. This method is quite useful, because it provides information on the thermal behavior of the cathode material up to 12 V. Similar approaches were reported to improve the electrochemical properties of the cathode materials by a sol–gel coating of  $\text{Al}_2\text{O}_3$  and  $\text{ZrO}_2$  [15–17]. However, its overcharge behavior was not yet reported despite its superior rate capability and cycle-life performance, compared to the bare cathodes.

In this paper, differences in the  $\text{Al}_2\text{O}_3$ - and  $\text{AlPO}_4$ -coated  $\text{LiCoO}_2$  are investigated for the electrochemical and thermal behavior.

## 2. Experimental

$\text{LiCoO}_2$  was prepared using  $\text{Co}_3\text{O}_4$  (with the average particle size of 2–3  $\mu\text{m}$ ) and finely ground  $\text{LiOH}\cdot\text{H}_2\text{O}$  powders as starting materials. They were mixed at a molar ratio of 1:1.05 and homogenized in an automatic mixer for 2 h. The mixture was heat-treated at 600 and 900  $^\circ\text{C}$  in an oxygen atmosphere for 6 and 24 h, respectively. The as-prepared  $\text{LiCoO}_2$  powders had an  $x=1.00$  in  $\text{Li}_x\text{CoO}_2$ . The  $\text{LiCoO}_2$  electrode powder with an average particle of size  $\sim 10\ \mu\text{m}$ , which was sampled from the batches sieving through a 500-mesh screen (26  $\mu\text{m}$ ), was used for the electrochemical tests. To obtain the sol–gel coating of  $\text{Al}_2\text{O}_3$  on  $\text{LiCoO}_2$ ,  $\text{Al(IV)ethylhexanoisopropoxide}$  ( $\text{Al}(\text{OOC}_8\text{H}_{15})_2(\text{OC}_3\text{H}_7)_2$ , 5 g) was dissolved in isopropanol, followed by continuous stirring for 20 h at 21  $^\circ\text{C}$ . After drying the  $\text{LiCoO}_2$  powders coated with Al alkoxide gel at 130  $^\circ\text{C}$ , the batch was fired at 700  $^\circ\text{C}$  for 5 h. Aluminum nitrate ( $\text{Al}(\text{NO}_3)_3\cdot 9\text{H}_2\text{O}$ , 3 g) and diammonium phosphate ( $(\text{NH}_4)_2\text{HPO}_4$ , 1 g) were dissolved in distilled water until a light white suspension solution (with  $\text{AlPO}_4$  nanoparticles) was observed. The  $\text{LiCoO}_2$  powders (100 g with the average particle size of  $\sim 10\ \mu\text{m}$ ) were then slowly added to the coating solution, and mixed until the final viscosity of the slurry reached  $\sim 100\ \text{P}$ . Subsequently, the slurry was poured into a tray, dried in an oven for 6 h at 130  $^\circ\text{C}$ , and annealed at 700  $^\circ\text{C}$  for 5 h in a furnace.

The cell standard capacity was set at 1600 mAh [cell size: 3.2 mm  $\times$  85 mm  $\times$  53 mm (thickness  $\times$  length  $\times$  width)]. The electrolyte for the coin-type half cells and the Li-ion

cells was 1 M  $\text{LiPF}_6$  with ethylene carbonate/diethylene carbonate/ethyl-methyl carbonate (EC/DEC/EMC) (30:30:40 vol.%). The coin-type half cells were initially cycled at a 0.1 C rate for two cycles, and continued to increase to 0.2 and 0.5 C rates for each cycle, followed by a 1 C rate afterwards, with 4.6 and 4.8 V charge-cutoffs. The discharge voltage was set to 3 V. Coin-type half cells containing Li metal anode were used for cycling tests with 4.6 and 4.8 V cutoffs. Cycling tests of the Li-ion cells between 3 and 4.5 V was performed with synthetic graphite. Rate capability tests of the coated cathodes was carried out using 1600 mAh Li-ion cell between 3 and 4.2 V with synthetic graphite anode at different C rates at room temperature. The same dimensional weight ratio of cathode to anode (1:1.06) was used for all the test cells. To determine the apparent Li diffusivities as a function of the cell potential, a galvanostatic intermittent titration technique (GITT) was used for the uncoated and  $\text{Al}_2\text{O}_3$ - and  $\text{AlPO}_4$ -coated  $\text{LiCoO}_2$  powders. The experimental methods for the DSC and 12 V overcharge tests were described elsewhere [18].

## 3. Results and discussion

A comparison of the transmission electron microscopy (TEM) images between the  $\text{Al}_2\text{O}_3$ - and  $\text{AlPO}_4$ -coated  $\text{LiCoO}_2$  particles is shown in Fig. 1. In both cases, the Al or P elements are distributed over the  $\text{LiCoO}_2$  surfaces. The possible formation of a solid solution from a reaction between the coating materials and Li (or even Co) during the heat treatment is not ruled out. X-ray photoelectron spectroscopy (XPS) was used to compare the bonding nature of the  $\text{Al}_2\text{O}_3$ - and  $\text{AlPO}_4$ -coated cathodes, as shown in Fig. 2. The binding energies of the Al 2p in the bulk  $\text{Al}_2\text{O}_3$  and  $\text{AlPO}_4$  were reported to be observed at  $\sim 74.7$  and 74.5 eV, respectively [19,20]. A peak in the  $\text{Al}_2\text{O}_3$ -coated  $\text{LiCoO}_2$  at  $\sim 71$  eV agrees with the metallic nature of Al. The variation in the binding energies of Al in the coated cathodes may be related to a Li (or even Co) reaction with the coating layer, and future study aimed at understanding the detailed microstructures of the nanoscale coating layer is currently underway.

Fig. 3 compares the voltage profile and cycle-life performance of bare, and  $\text{Al}_2\text{O}_3$ - and  $\text{AlPO}_4$ -coated cathodes between 4.6 and 3 V. The initial capacity and cycle-life performance of the  $\text{Al}_2\text{O}_3$ -coated cathode are similar to those in the  $\text{AlPO}_4$ -coated samples. However, increasing the charge voltage from 4.6 to 4.8 V leads to a drastic difference between these two cathodes, as shown in Fig. 4. Even though the charge capacities of both cathodes are similar to each other (244 and 247  $\text{mAh g}^{-1}$  for  $\text{Al}_2\text{O}_3$ - and  $\text{AlPO}_4$ -coated  $\text{LiCoO}_2$ , respectively), the discharge capacity is obviously different:  $\text{Al}_2\text{O}_3$ - and  $\text{AlPO}_4$ -coated  $\text{LiCoO}_2$  show 220 and 233  $\text{mAh g}^{-1}$ , respectively. Cobalt dissolution into the solution is coupled with the release of lithium and oxygen, resulting in structural degradation [21]. The Co dissolution rate in the  $\text{Al}_2\text{O}_3$ -coated cathodes was four times higher than that in

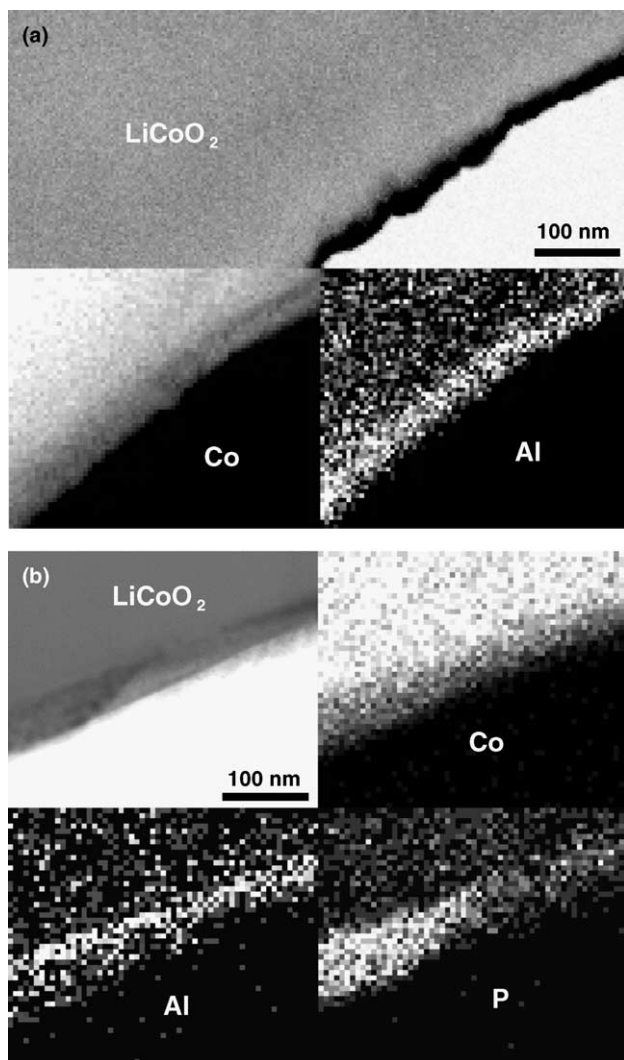


Fig. 1. TEM images of: (a)  $\text{Al}_2\text{O}_3$ -coated and (b)  $\text{AlPO}_4$ -coated  $\text{LiCoO}_2$ . Energy dispersive spectroscopy confirms the existence of either Al or P on the surface and Co in the interior of the powder.

the  $\text{AlPO}_4$ -coated cathodes after the initial 0.1 C rate cycling (between 4.8 and 3 V), and the concentrations were  $\sim 160$  and 40 ppm for  $\text{Al}_2\text{O}_3$ - and  $\text{AlPO}_4$ -coated  $\text{LiCoO}_2$ , respectively. This affected the cycling stability of the coated cathode [22]. The  $\text{AlPO}_4$ -coated  $\text{LiCoO}_2$  exhibits superior capacity retention after 46 cycles (at a 1 C rate) showing  $\sim 82\%$  capacity retention, while that of the  $\text{Al}_2\text{O}_3$ -coated cathode shows  $\sim 68\%$ . This is due to the structural degradation of the  $\text{LiCoO}_2$  from Co dissolution, which was  $\sim 450$  and 160 ppm for the  $\text{Al}_2\text{O}_3$ - and  $\text{AlPO}_4$ -coated cathodes, respectively. These results confirm that the  $\text{AlPO}_4$ -coating layer is chemically more stable at the 4.8 V electrochemical window compared to the  $\text{Al}_2\text{O}_3$  coating.

This is supported by the cycle-life performance in the Li-ion cells (with carbon as an anode) containing  $\text{Al}_2\text{O}_3$ - and  $\text{AlPO}_4$ -coated  $\text{LiCoO}_2$  cathodes. As shown in Fig. 5 with a charge-cutoff voltage of 4.5 V at the 1 C rate, the capacity-fading rate of the  $\text{Al}_2\text{O}_3$ -coated  $\text{LiCoO}_2$  is similar to that of

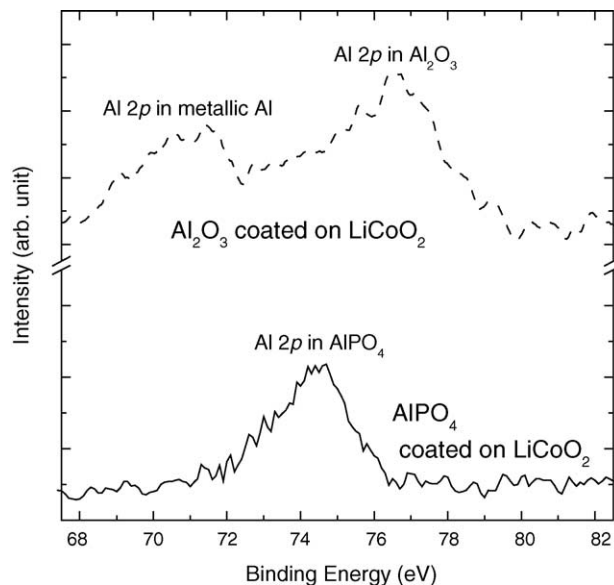


Fig. 2. XPS spectra of the Al 2p binding energies from the  $\text{Al}_2\text{O}_3$  (dashed line) and  $\text{AlPO}_4$  (solid line) nanoscale-coating layer on  $\text{LiCoO}_2$ .

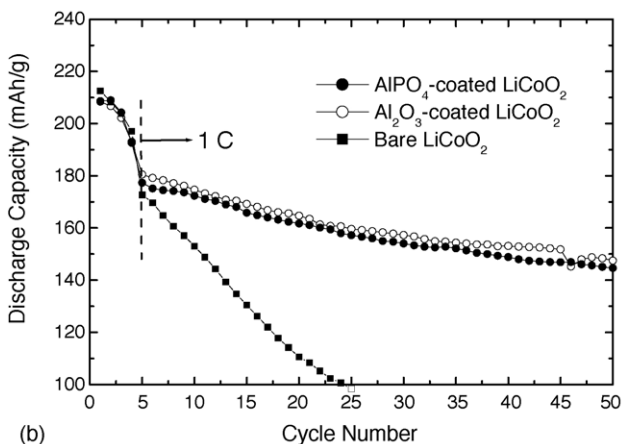
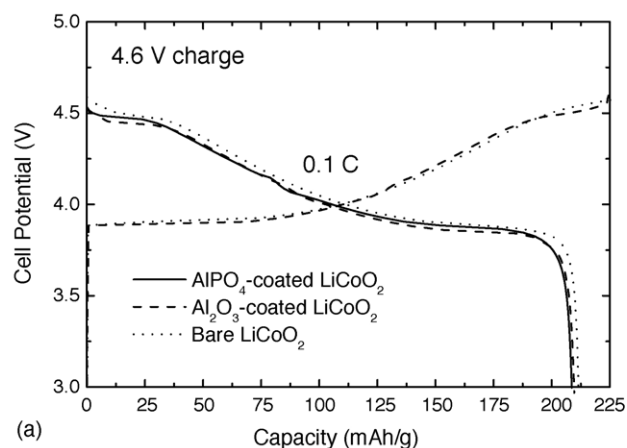
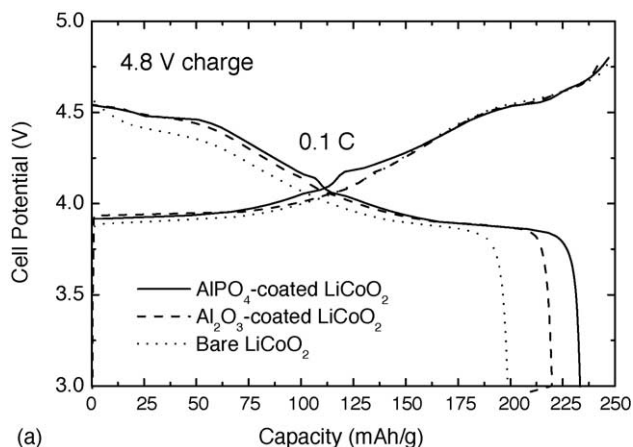
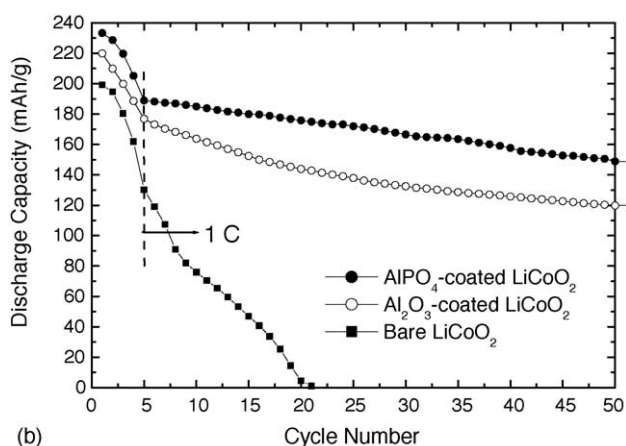


Fig. 3. (a) Voltage profiles and (b) capacity retention of bare, and  $\text{Al}_2\text{O}_3$ - and  $\text{AlPO}_4$ -coated  $\text{LiCoO}_2$  cathodes in the coin-type half cells (Li as an anode) with a charge voltage of 4.6 V (pre-cycled at rates of 0.1 C for the initial two cycles, and 0.2 and 0.5 C each for the next two cycles).



(a)



(b)

Fig. 4. (a) Voltage profiles and (b) capacity retention of bare, and  $\text{Al}_2\text{O}_3$ - and  $\text{AlPO}_4$ -coated  $\text{LiCoO}_2$  cathodes in the coin-type half cells with a charge voltage of 4.8 V (pre-cycled at the rates of 0.1 C for the initial two cycles, and 0.2 and 0.5 C each for the next two cycles).

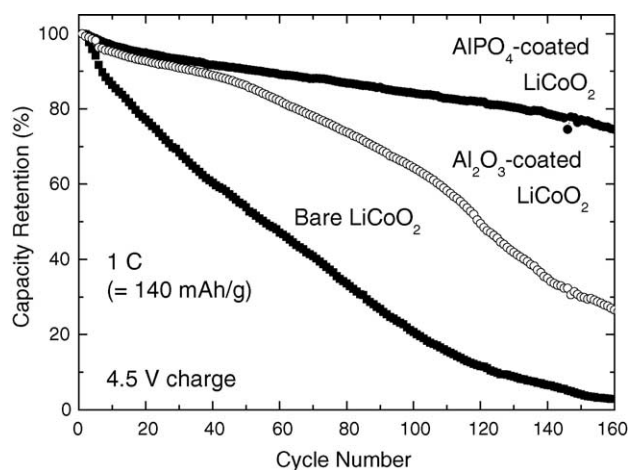
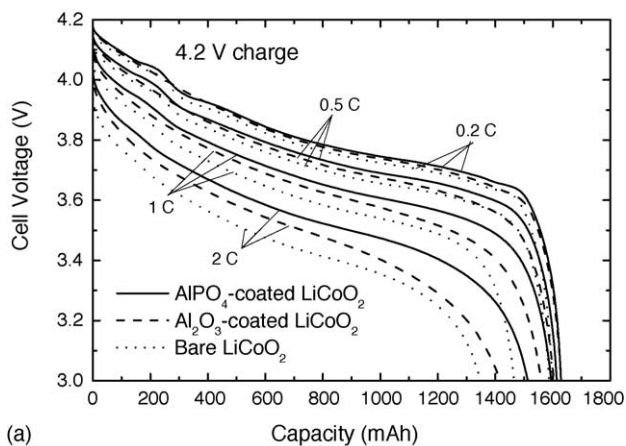
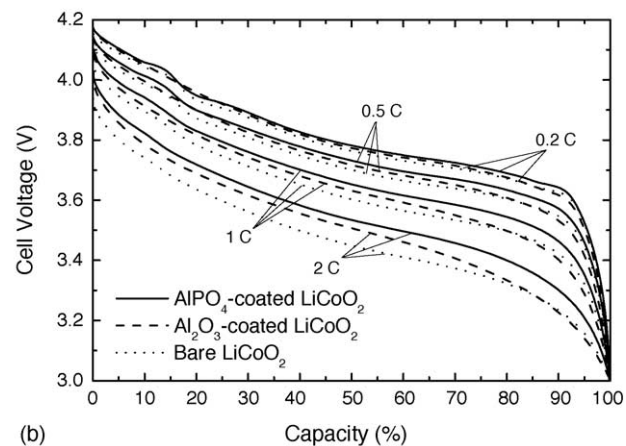


Fig. 5. Capacity retention of bare, and  $\text{Al}_2\text{O}_3$ - and  $\text{AlPO}_4$ -coated  $\text{LiCoO}_2$  cathodes in the Li-ion cells (with a carbon anode) with a charge-cutoff voltage of 4.5 V.



(a)



(b)

Fig. 6. Plots of: (a) rate capabilities and (b) normalized capacity of bare, and  $\text{Al}_2\text{O}_3$ - and  $\text{AlPO}_4$ -coated  $\text{LiCoO}_2$  cathodes in the Li-ion cells (with carbon anode) with a charge-cutoff voltage of 4.2 V.

the  $\text{AlPO}_4$ -coated  $\text{LiCoO}_2$  for the initial  $\sim 40$  cycles. However, its capacity rapidly decreases to  $\sim 27\%$  after 160 cycles (between 4.5 and 2.75 V), while the capacity-fading rate from the  $\text{AlPO}_4$ -coated cathode is much slower, showing  $\sim 75\%$  after 160 cycles. The amount of Co dissolution after 40 cycles in the cell containing the  $\text{Al}_2\text{O}_3$ -coated cathode is similar to that in the  $\text{AlPO}_4$ -coated cathode, showing  $\sim 70$  ppm. However, the amount of Co dissolution from the  $\text{Al}_2\text{O}_3$ -coated cathode increased to  $\sim 3200$  ppm after 160 cycles. (The Co dissolution in  $\text{AlPO}_4$ -coated cathode was  $\sim 300$  ppm.) The result suggests that the  $\text{Al}_2\text{O}_3$ -coating layer is relatively stable during the initial cycles, but chemically less stable either for higher voltage or for a long-time exposure to the electrolyte. Actually, the dissolved amount of Al into the electrolyte in the  $\text{Al}_2\text{O}_3$ -coated cathode was  $\sim 980$  ppm after 160 cycles, compared to the  $\sim 100$  ppm dissolution of Al in the  $\text{AlPO}_4$ -coated one.

Fig. 6(a) shows the rate capability of bare, and  $\text{Al}_2\text{O}_3$ - and  $\text{AlPO}_4$ -coated  $\text{LiCoO}_2$  in Li-ion cells at the rates of 0.2, 0.5, 1, and 2 C between 4.2 and 3 V. Capacity-retention rate of the  $\text{AlPO}_4$ -coated  $\text{LiCoO}_2$  is enhanced, compared to the  $\text{Al}_2\text{O}_3$ -coated  $\text{LiCoO}_2$  with an increasing current rate: the

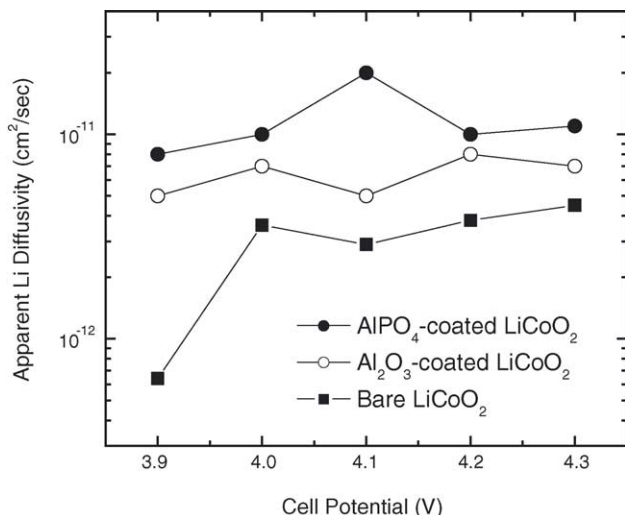


Fig. 7. Apparent Li-ion diffusivity vs. charging voltage in bare, and  $\text{Al}_2\text{O}_3$ - and  $\text{AlPO}_4$ -coated  $\text{LiCoO}_2$  after four precycles.

former showing 8% larger capacity retention than the latter at a 2 C rate. Fig. 6(b) shows the voltage profiles of bare, and  $\text{Al}_2\text{O}_3$ - and  $\text{AlPO}_4$ -coated  $\text{LiCoO}_2$  at 0.2, 0.5, 1, and 2 C rates between 4.2 and 3 V as a function of the normalized capacity. Since other factors, such as the carbon anode and electrolytes are fixed in the Li-ion cells, the change in the voltage profile should be affected by the coating layer. The enhanced voltage profiles of the  $\text{AlPO}_4$ -coated cathode compared to  $\text{Al}_2\text{O}_3$ -coated one at different C rates are believed to be due to the higher apparent Li diffusivity in the  $\text{LiCoO}_2$  powder by the  $\text{AlPO}_4$  coating. Fig. 7 shows the higher apparent Li diffusivity in the  $\text{AlPO}_4$ -coated cathode over the  $\text{Al}_2\text{O}_3$ -coated cathode (after four precycles). It was reported that the apparent Li diffusivity of the coated cathode at the first cycle was smaller than the bare one, and got higher upon further cycling [23].

The DSC scans of the bare,  $\text{Al}_2\text{O}_3$ -, and  $\text{AlPO}_4$ -coated  $\text{LiCoO}_2$  electrodes are shown in Fig. 8. The exothermic peak

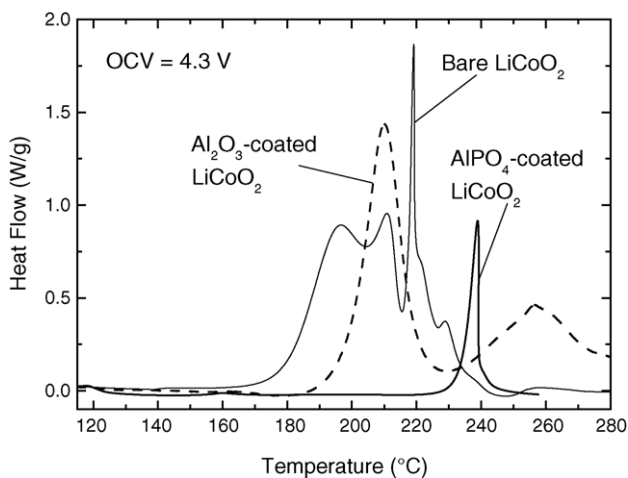


Fig. 8. DSC scans of bare, and  $\text{Al}_2\text{O}_3$ - and  $\text{AlPO}_4$ -coated  $\text{LiCoO}_2$  after 4.3 V charge. The scan rate was  $3^\circ\text{C min}^{-1}$ .

area indicates the amount of heat generation (related to oxygen generation) from the decomposed cathode after a reaction with the electrolyte. The onset temperature of oxygen evolution from the cathode in the bare electrode is  $\sim 170^\circ\text{C}$ , but improved to  $\sim 190^\circ\text{C}$  in the  $\text{Al}_2\text{O}_3$ -coated cathode. However, the  $\text{AlPO}_4$ -coated electrode shows the highest onset temperature among the other electrodes ( $\sim 230^\circ\text{C}$ ), indicating that the  $\text{AlPO}_4$ -coating layer effectively retards the initiation of the oxygen generation from the cathode, with a much lower amount of exothermic-heat release.

In order to investigate the 12 V overcharge behavior of the  $\text{Al}_2\text{O}_3$ - and  $\text{AlPO}_4$ -coated  $\text{LiCoO}_2$ , the Li-ion cells containing these cathodes are overcharged to 12 V, and held at that voltage until the applied current decreases to  $\sim 30$  mA. Previously, it was suggested that the short circuit at 12 V resulted from the direct contact between the anode and cathode due to the separator shrinkage, accompanying a rapid temperature upsurge, which induces a thermal runaway according to the stability of the cathode [5]. Fig. 9 compares the 12 V overcharge behaviors of the Li-ion cells containing the bare, and  $\text{Al}_2\text{O}_3$ - and  $\text{AlPO}_4$ -coated  $\text{LiCoO}_2$  cathodes.

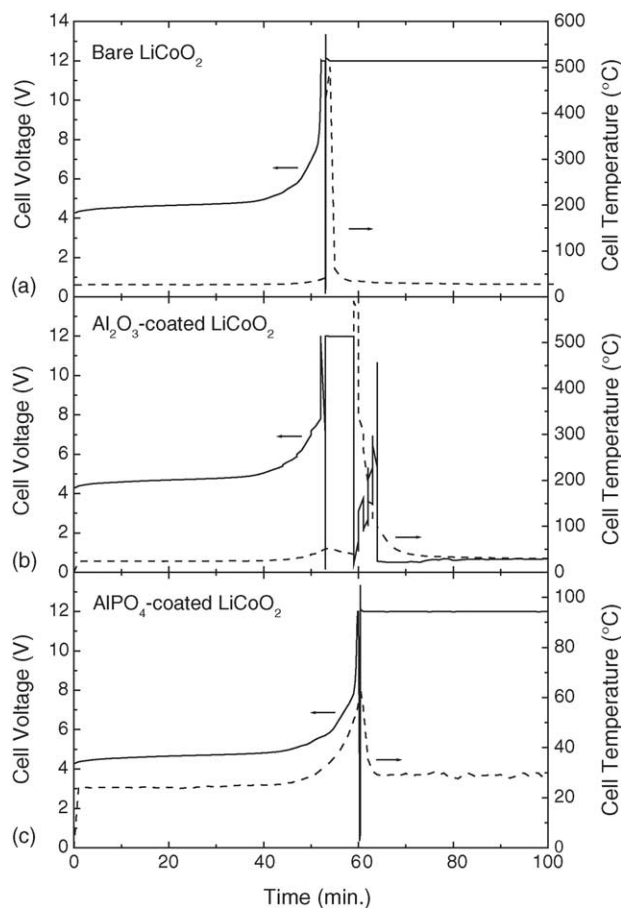


Fig. 9. (a–c) Voltage (solid lines) and temperature (dotted lines) profiles of the cells with bare, and  $\text{Al}_2\text{O}_3$ - and  $\text{AlPO}_4$ -coated  $\text{LiCoO}_2$  cathode as a function of time, showing the breakdown of the cells by one full short circuit. All the cells were first charged to 4.2 V, and overcharged to 12 V at a rate of 1 C, then held at that voltage for  $\sim 50$  min.

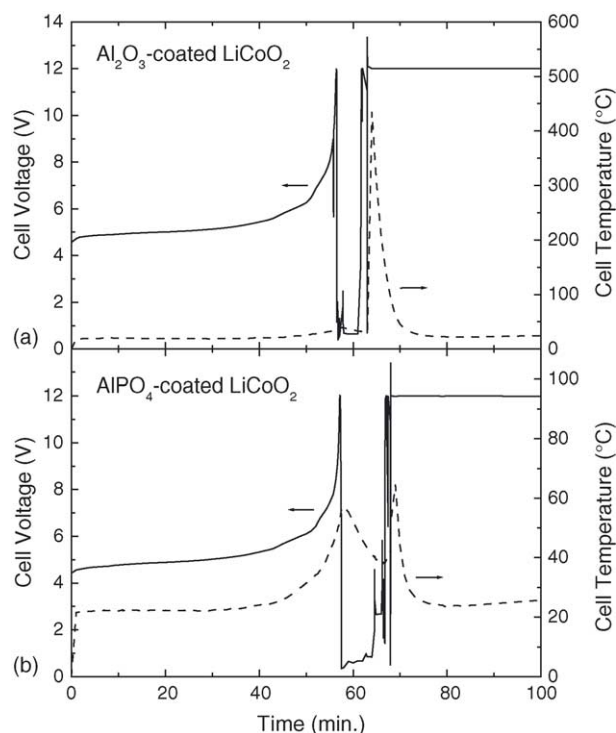


Fig. 10. (a and b) Voltage (solid lines) and temperature (dotted lines) profiles of the cells with the  $\text{Al}_2\text{O}_3$ - and  $\text{AlPO}_4$ -coated  $\text{LiCoO}_2$  cathode as a function of time, showing breakdown of the cells by another internal short circuit after the first internal short circuit. The sequential local short-circuit phenomenon was not observed in bare cathode materials. The charging conditions were same as in Fig. 9.

When a separator melts at  $\sim 120^\circ\text{C}$ , it triggers large heat output induced by an internal short circuit. After spiking to 12 V, the cell containing the  $\text{Al}_2\text{O}_3$ -coated cathode shows thermal runaway with the surface temperature of the cell over  $\sim 500^\circ\text{C}$ . In this condition, the cell was burnt off completely. This behavior is quite similar to that observed in the bare cell [5]. Even though the cell with an  $\text{AlPO}_4$  nanoparticle-coated  $\text{LiCoO}_2$  cathode has a short circuit, the temperature increases to only  $\sim 60^\circ\text{C}$  without burning the cell. All these are related to the Co dissolution, the cycle-life performance, and the DSC results. Another interesting feature observed during the 12 V overcharging is that the cell voltage recovers to 12 V, followed by another internal short circuit after showing the first internal short circuit, as shown in Fig. 10. In this case, the cell containing the  $\text{Al}_2\text{O}_3$ -coated  $\text{LiCoO}_2$  cathode exhibits the maximum surface temperature of  $\sim 500^\circ\text{C}$ . However,  $\text{AlPO}_4$ -coated  $\text{LiCoO}_2$  shows a maximum temperature of only  $\sim 60^\circ\text{C}$ , indicating that the  $\text{AlPO}_4$ -coating layer is still stable after the successive short circuits in contrast to the  $\text{Al}_2\text{O}_3$ -coating layer.

#### 4. Conclusions

With a nanoscale coating of  $\text{Al}_2\text{O}_3$  and  $\text{AlPO}_4$  on the  $\text{LiCoO}_2$  cathode powders, the electrochemical and thermal

stability strongly depended on the nature of the coating materials. The  $\text{AlPO}_4$ -coated cathode exhibited a superior cycle-life performance at a 4.8 V charge-cutoff, an improved onset temperature for oxygen evolution, and no fire and explosion from the 12 V overcharge safety tests. This is probably because the  $\text{Al}_2\text{O}_3$ -coating layer diminishes and cannot prevent Co dissolution into the electrolyte during overcharging or at an elevated temperature, which is in contrast to the  $\text{AlPO}_4$ -coated cathode.

#### Acknowledgments

This work was supported by Kumoh National Institute of Technology, the Basic Research Program (R01-2004-000-10173-0) of KOSEF, the National R&D Program of the Ministry of Science and Technology, and KOSEF through the Research Center for Energy Conversion and Storage at Seoul National University.

#### References

- [1] Guideline for the Safety Evaluation of Secondary Lithium Cells, Japan Battery Association, 1997.
- [2] A Safety Standard for Lithium Batteries, UL1642, third ed., Underwriters Laboratories, 1995.
- [3] Laptop Batteries are Linked to Fire Risk, New York Times, March 15, 2001; U.S. Consumer Product Safety Commission (<http://www.cpsc.gov/cpscpub>).
- [4] S.C. Levy, P. Bro, Battery Hazards and Accident Prevention, Plenum Press, NY, 1994.
- [5] J. Cho, Y.-W. Kim, B. Kim, J.-G. Lee, B. Park, *Angew. Chem. Int. Ed.* 42 (2003) 1618.
- [6] R.A. Leising, M.J. Palazzo, E.S. Takeuchi, K.J. Takeuchi, *J. Electrochem. Soc.* 148 (2001) A838.
- [7] H. Maleki, S.A. Hallaj, J.R. Selman, R.B. Dinwiddie, H. Wang, *J. Electrochem. Soc.* 146 (1999) 947.
- [8] A. Duaquier, F. Disma, T. Bowmer, A.S. Gozdz, G.G. Amatucci, J.-M. Tarascon, *J. Electrochem. Soc.* 145 (1998) 12.
- [9] H. Maleki, G. Deng, A. Anani, J. Howard, *J. Electrochem. Soc.* 146 (1999) 3224.
- [10] N. Takami, H. Inagaki, H. Ishii, R. Ueno, R.M. Kanda, IMLB11: 11th International Meeting on Lithium Batteries, June 23–28, 2002, Monterey, CA, U.S.A., 2002.
- [11] K. Xu, M.S. Ding, S. Zhang, J. Allen, T.R. Jow, *J. Electrochem. Soc.* 149 (2002) A622.
- [12] S.C. Narang, S.C. Ventura, B.J. Dougherty, M. Zhao, M.S. Smedley, G. Koolpe, U.S. Patent 5830660.
- [13] M. Adachi, K. Tanaka, K. Sekai, *J. Electrochem. Soc.* 146 (1999) 1256.
- [14] X. Wang, E. Yasukawa, S.J. Kasuya, *J. Electrochem. Soc.* 148 (2001) A1058.
- [15] J. Cho, Y.J. Kim, T.-J. Kim, B. Park, *Angew. Chem. Int. Ed.* 40 (2001) 3367.
- [16] J. Cho, Y.J. Kim, T.-J. Kim, B. Park, *Chem. Mater.* 13 (2001) 18.
- [17] J. Cho, Y.J. Kim, B. Park, *Chem. Mater.* 12 (2000) 3788.
- [18] J. Cho, J.-G. Lee, B. Kim, B. Park, *Chem. Mater.* 15 (2003) 3190.
- [19] J. Chastain, R.C. King Jr. (Eds.), Handbook of X-ray Photoelectron Spectroscopy, Physical Electronics Inc., MN, 1995.

- [20] J.A. Rotole, P.M.A. Sherwood, *Surf. Sci. Spectrom.* 5 (1998) 60.
- [21] G.G. Amatucci, J.M. Tarascon, L.C. Klein, *Solid State Ionics* 83 (1996) 167.
- [22] Y.J. Kim, J. Cho, T.-J. Kim, B. Park, *J. Electrochem. Soc.* 150 (2003) A1723.
- [23] Y.J. Kim, H. Kim, B. Kim, D. Ahn, J.-G. Lee, T.-J. Kim, D. Son, J. Cho, Y.-W. Kim, B. Park, *Chem. Mater.* 15 (2003) 1505.